Proceedings, Bicycle and Motorcycle Dynamics 2010
Symposium on the Dynamics and Control of Single Track Vehicles,
20 - 22 October 2010, Delft, The Netherlands

A Virtual Rider for Reproducing Experimental Manoeuvres

M. Massaro, V. Cossalter, R. Lot

Dept. of Innovation in Mechanics and Management
University of Padua
Via Venezia 1, 35131 Padova, Italy
e-mail: {matteo.massaro|vittore.cossalter|roberto.lot}@unipd.it

ABSTRACT

The control of two-wheeled vehicles represents a challenging task. Indeed the stability of a bike is characterized by vibration modes which significantly change their behaviour with speed and acceleration and may become unstable under certain motion condition. This paper presents a virtual rider model which accounts for these effects by updating at each instant the control action, based on the information of the approaching road section and the current vehicle state. This approach mimics the real rider behaviour, who looks ahead, learning a portion of the track, continuously using this information to decide when/how to steer and accelerate. As an example of application, the virtual rider is used to reproduce a lap of the Mugello circuit (Italy): the real motorcycle speed and roll angle are used as target motion by the virtual rider, which effectively controls the vehicle with longitudinal acceleration up to *1 g* and roll angle up to *50°*.

Keywords: motorcycle dynamics, virtual rider, virtual driver, control, stability, multiboby.

1 INTRODUCTION

Since two-wheeled vehicles are intrinsically unstable, see e.g. [1]-[3], a virtual rider model is required in addition to the vehicle model to numerically simulate the system dynamics. This is a substantial difference with respect to car/truck simulation, where the vehicle model can be used to reproduce many typical open-loop manoeuvres (e.g. steering wheel step) without the need of a virtual driver model.

Different control strategies have been proposed in the past years, and the control of single-track vehicles remains an open research field. Nonlinear optimal control theory has proven successful, [4]-[5], but computational reasons make this approach not appealing for complex multiboby model. PID approaches have demonstrated effective for constant speed or slowly varying manoeuvres only, [6],[7]. Optimal linear time invariant controllers have been used for constant speed manoeuvres [8] and speed control [9]. The linear optimal control theory designed on a very simple motorcycle model has been used to control a complex multiboby code in [10] and a recent discussion on linear predictive control for motorcycle with constant speed simulations is devised in [11]. Most of these works deal with constant speed or slowly varying speed manoeuvres.

In [12] a virtual rider which controls the bike with both strong longitudinal and lateral accelerations has been presented. Such performance is achieved by updating at each instant the control action based on the information of the approaching road section and the current vehicle state. In more detail, the approach is based on the predictive control theory framework. At each step the virtual rider computes the control action using an appropriate linear model which is derived from the full nonlinear multiboby model. The virtual rider proved effective for simulating the nonlinear motorcycle model while performing simple yet demanding entering/exiting a curve manoeuvres, with longitudinal acceleration up to *1 g* and roll angles up to *50°*. The target motion is defined in terms of speed and roll angle. The choice of these targets is motivated by

the demand of motorcycle and tyre companies to simulate cornering manoeuvres at variable speed using multiboby codes.

This paper extends the results of [12] from two points of view: 1) the virtual rider model is applied to the very detailed motorcycle model presented in [13], in order to prove the effectiveness of the approach in guiding complex models; 2) the virtual rider is employed to reproduce complex experimental manoeuvres (instead of simple entering/exiting a curve while accelerating/braking manoeuvres), in order to test the virtual rider capability in reproducing real rider behaviour. As an example of application, the virtual rider is used to reproduce a lap of the Mugello circuit (Italy): the real bike speed and roll angle are used as target motion by the virtual rider, which controls the vehicle with strong longitudinal acceleration and lateral acceleration.

The paper is structured as follows: in section 2 the multiboby model used for simulation is briefly described, in section 3 the virtual rider is presented and in section 4 the performance of the virtual rider while reproducing a real manoeuvres are analyzed.

2 MOTORCYCLE MODEL

Several works on motorcycle dynamics have been presented in the past years and different mathematical models have been proposed, [2],[3],[13]-[18]. Among them, this paper employed the advanced and validated multiboby code presented in [13].

The motorcycle model is made of the 9 rigid bodies and as many body reference frame, see Figure 1: the chassis, which consists of two bodies elastically connected (the rear chassis, i.e. the part of the chassis near the rear suspension pivots, plus the front chassis, near the steering plate), the front frame (i.e. the handlebar and the upper part of the front suspension), the front and rear wheels, the front unsprung mass (i.e. the lower part of the front suspension, the front brake caliper, etc.) and the rear unsprung mass (e.g. the swingarm). The rider is modelled with two additional rigid bodies: the lower rider (from feet to hip) and the upper rider (from hip to head). The model has 11 degrees of freedom (DOF) related to the gross motion of the motorcycle: the position and orientation of the chassis, the steer rotation, the suspensions travels and the wheels rotations. Several additional DOF are included to account for the vehicle flexibilities, and the user may decide either to include in the model or to lock any of these structural DOF, increasing the number of DOF from 11 (rigid bodies only) to 29 (all standard flexibilities included). For the motorcycle considered herein, the structural lateral flexibility of the front frame has been included: this is essential for a proper modelling of the vehicle stability, see e.g. [18].

The motorcycle inputs are the steering torque τ, the rear wheel propulsive/brake torque η, and the front wheel brake torque ρ.

The road-tyre contact forces are computed according to the well know Magic Formula for motorcycle. Two approaches are available for the force coupling: the Similarity Method and the Loss Functions Method, see [3]. The tyre model takes into account also the carcass compliance and damping by means of the lateral ζ_L, radial ζ_R, and the tangential ξ deflections.

The main vehicle parameters are reported in appendix.

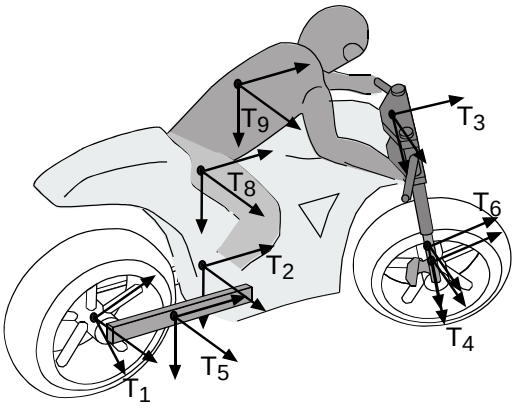

Figure 1. Motorcycle model used for simulation.

3 VIRTUAL RIDER MODEL

The virtual rider is designed to guide the continuous nonlinear motorcycle model described in section 2 along generic target roll and target speed profiles, and it is based on the discrete predictive control theory framework. In particular, at each instant t_i the nonlinear motorcycle model is linearized about the target motion at that instant, i.e. target roll $\phi(t_i)$ and target speed $v(t_i)$, and the resulting linear model is used for the synthesis of the virtual rider. This virtual rider is employed to simulate the nonlinear model for the next simulation step, i.e. from t_i to $t_i+\Delta$, where Δ is the integration time step. The procedure is repeated at each step, and therefore the virtual rider uses always an appropriate linear model for the computation of the control action, i.e. when the vehicle is close to straight motion the linear model obtained in the straight motion condition is used, when the vehicle is cornering the linear model in cornering condition is used, etc. More precisely, the virtual rider synthesis is computed with time step T, while the nonlinear model is simulated with time step Δ, with $T>\Delta$ for efficiency purpose.

In more detail, at each synthesis step k, which corresponds to the simulation time $t_i=(k-1)T$, the nonlinear model is solved for equilibrium in the corresponding target motion condition $\mathbf{r}(k)$

$$\mathbf{r}(k) = \begin{Bmatrix} \phi(k) \\ v(k) \end{Bmatrix} \tag{1}$$

to give the equilibrium state $\mathbf{x}_0(k)$ and equilibrium input $\mathbf{u}_0(k)$. Afterwards, the nonlinear model is linearized about $\mathbf{x}_0$, $\mathbf{u}_0$ and converted into its discrete formulation with the discretization time step T to give:

$$\begin{cases} \overline{\mathbf{x}}(k+1) = \mathbf{A}(k)\overline{\mathbf{x}}(k) + \mathbf{B}(k)\overline{\mathbf{u}}(k) \\ \overline{\mathbf{y}}(k) = \mathbf{C}(k)\overline{\mathbf{x}}(k) \end{cases} \tag{2}$$

where $\mathbf{A}(k), \mathbf{B}(k), \mathbf{C}(k)$ are the discrete state space matrices, $\overline{\mathbf{x}}(k)$ is the vector of the state variables, $\overline{\mathbf{u}}(k)$ is the input vector and $\overline{\mathbf{y}}(k)$ is the vector of the observed variables (roll ϕ and speed v). More precisely, $\overline{\mathbf{x}}$ is the difference between the state variables of the nonlinear system $\mathbf{x}_{NL}$ and the steady state variables $\mathbf{x}_0$, $\overline{\mathbf{u}}$ is the difference between the inputs of the nonlinear system $\mathbf{u}_{NL}$ and the steady state inputs $\mathbf{u}_0$, $\overline{\mathbf{y}}$ is the difference between the nonlinear system observed variables $\mathbf{y}_{NL}$ and the target motion $\mathbf{r}(k)$.

The predictive approach requires the definition of a preview horizon, i.e. the number of steps N ahead of the vehicle (corresponding to a preview time $T_p=NT$) where the motion is predicted and used for the synthesis of the controller, and the cost function V which will be used for the optimization:

$$V(k) = \left\| \overline{\mathbf{Y}}(k) - \overline{\mathbf{T}}(k) \right\|_{\mathbf{Q}}^2 + \left\| \overline{\mathbf{U}}(k) \right\|_{\mathbf{R}}^2 \tag{3}$$

The cost function V accounts for the tracking error ($\left\| \overline{\mathbf{Y}}(k) - \overline{\mathbf{T}}(k) \right\|_{\mathbf{Q}}^2$, with $\mathbf{Q}$ weight matrix) and the input effort ($\left\| \overline{\mathbf{U}}(k) \right\|_{\mathbf{R}}^2$, with $\mathbf{R}$ weight matrix). In more detail:

$$\overline{\mathbf{Y}}(k) = \begin{Bmatrix} \overline{\mathbf{y}}(k+1) \\ \overline{\mathbf{y}}(k+2) \\ \vdots \\ \overline{\mathbf{y}}(k+N) \end{Bmatrix} \quad \overline{\mathbf{T}}(k) = \begin{Bmatrix} \mathbf{r}(k+1) - \mathbf{r}(k) \\ \vdots \\ \mathbf{r}(k+N) - \mathbf{r}(k) \end{Bmatrix} \quad \overline{\mathbf{U}}(k) = \begin{Bmatrix} \overline{\mathbf{u}}(k) \\ \overline{\mathbf{u}}(k+1) \\ \vdots \\ \overline{\mathbf{u}}(k+N-1) \end{Bmatrix} \tag{3}$$

It can be shown, see [12],[19], that the optimal control input at step k is:

$$\overline{\mathbf{u}}_{opt}(k) = \mathbf{K}(k) \begin{Bmatrix} \overline{\mathbf{x}}(k) \\ \overline{\mathbf{T}}(k) \end{Bmatrix} \tag{4}$$

and therefore the nonlinear control input which is used to guide the nonlinear motorcycle model is:

$$\begin{Bmatrix} \tau(k) \\ \eta(k) \\ \rho(k) \end{Bmatrix} = \mathbf{u}_0(k) + \overline{\mathbf{u}}_{opt}(k) \tag{3}$$

4 NONLINEAR SIMULATION

In this section the virtual rider described in section 3 is used to control the nonlinear motorcycle model described in section 2. The target motion is defined by the target roll angle and target speed logged from a real bike running on the Mugello circuit (Italy). The telemetry signals have been low passed in order to prevent the virtual rider from following the noise instead of the actual vehicle motion.

The preview horizon used by the virtual rider is set to T_p=*2.00 s*, the virtual rider synthesis is computed with time step *T=0.10 s*, the continuous nonlinear motorcycle model is simulated with time step *Δ=0.02 s*, the costs associated to the tracking error are $q_\phi = 10^7$ and $q_v = 10^2$, while the costs associated to the inputs are $r_\tau = 1$, $r_\eta = 10^2$ and $r_\rho = 10^{12}$. From the practical point of view the virtual rider adds a corrections to the steady state steering torque and rear wheel torque, while the front wheel torque has always the steady state value. The steady state inputs are computed at the target roll angle, target speed and target longitudinal acceleration (derived from the speed profile). It is worth noting that, since the motorcycle can brake with both front and rear wheel, the same deceleration may be performed with many different braking ratios, e.g. only front brake, only rear brake, 50% front brake and 50% rear brake, etc. It has been chosen to use an ideal braking ratio which engages the longitudinal adherence of both tyres equally, see [20]. Note that the ideal braking ratio changes with longitudinal acceleration: in particular in extreme braking condition almost only the front wheel torque is employed, because the rear tyre normal load is almost null due to the load transfer, while in mild braking condition

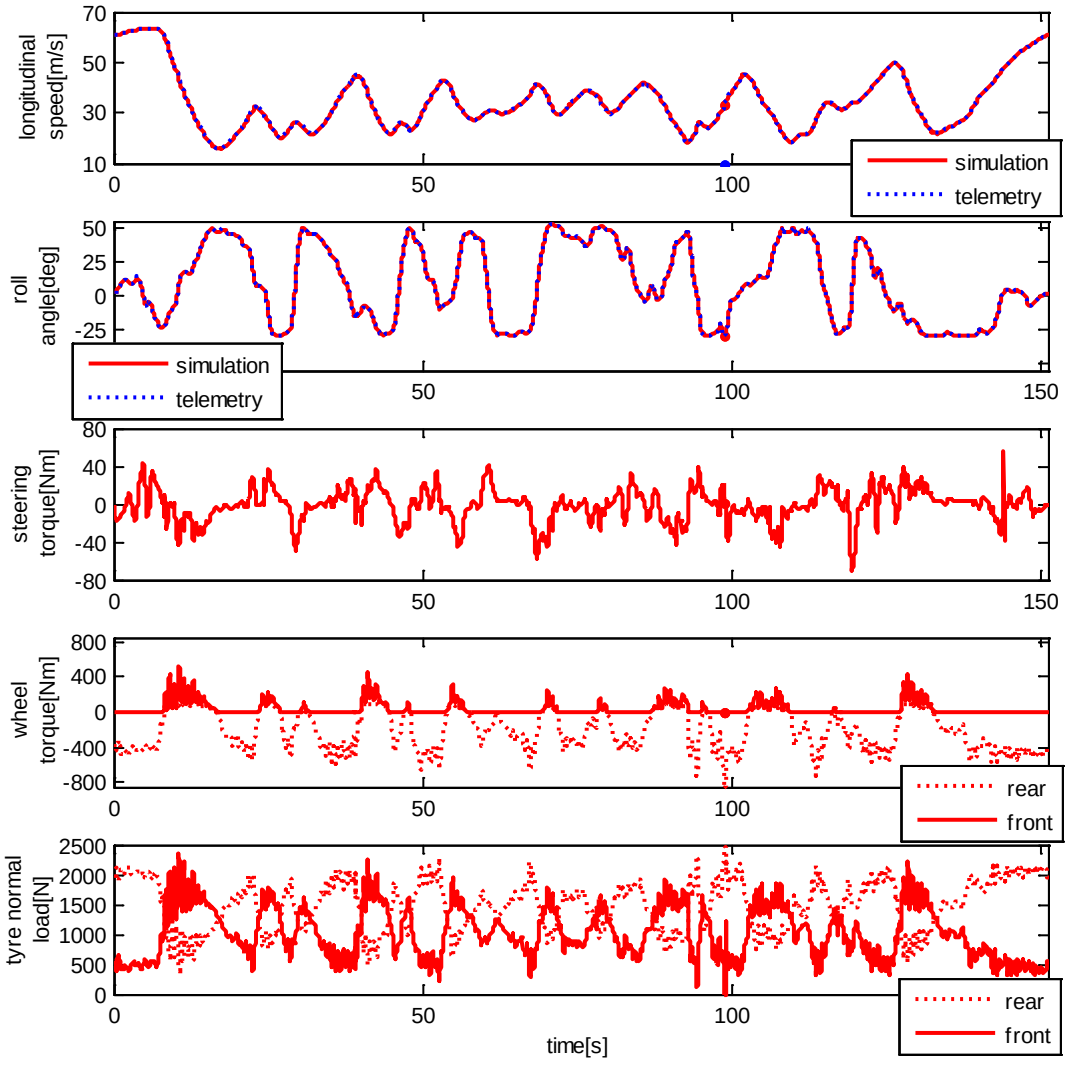

Figure 2. Simulation results (multiboby model with virtual rider, red lines) and telemetry logged from the real bike (blue lines).

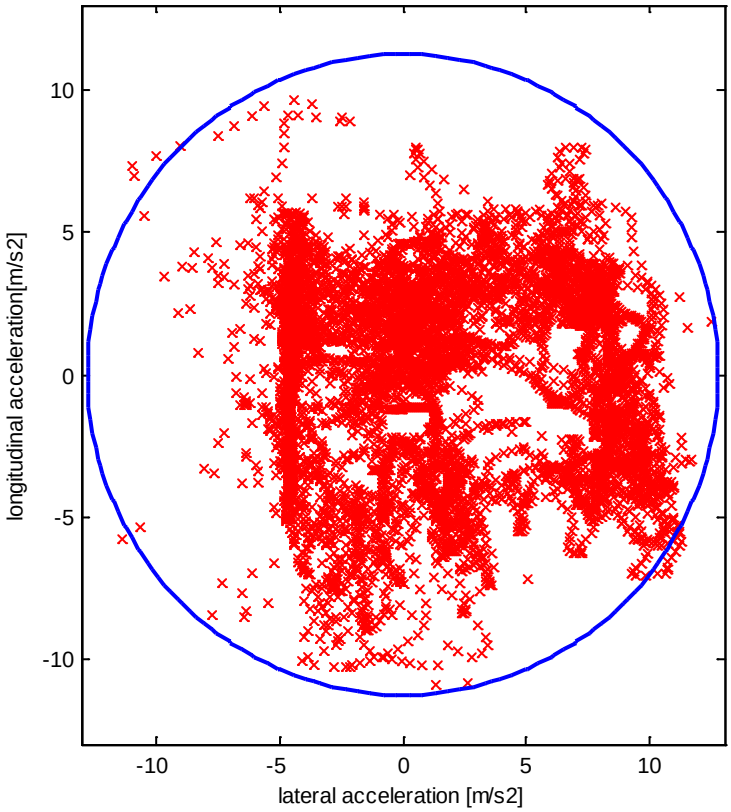

Figure 3. G-G diagram of the simulated manoeuvres.

the front and rear brakes are equally engaged.

Figure 2 depicts the simulation results in terms of speed, roll angle, steering torque, wheels torque and tyres normal load. It is worth noting that the tracking is almost perfect, both in terms of speed and roll angle. Note also that the roll angle exceeds *50°* in several points and that the longitudinal acceleration reaches *1 g*. The steering torque effort is in the range *-70..55 Nm*, the maximum front brake torque is *516 Nm*, the maximum rear brake torque is *98 Nm* and the maximum propulsive torque at the rear wheel is *-871 Nm*. Note that the tyre normal load fluctuation is significant, ranging from *0* to *2500 N*.

Figure 3 shows the G-G diagram for the manoeuvres simulated. From the inspection of the plot it is clear that both the longitudinal and lateral accelerations are significant, the maximum lateral acceleration being reached on right curves and the maximum longitudinal accelerations being reached while braking. Moreover there are several points where the virtual rider controls the vehicle with combined lateral and longitudinal acceleration (see in particular lower right area of Figure 3, which indicates right cornering while braking). For an analytical interpretation of motorcycles G-G diagrams see [21].

From the considerations above, it is concluded that the virtual rider presented herein can be used to simulate with multiboby codes the dynamics of real rider-vehicle systems.

4 CONCLUSIONS

An advanced virtual rider which is able to reproduce experimental manoeuvres in terms of roll angle and speed has been presented. The virtual rider has been implemented in a validated and detailed motorcycle multiboby code and its performance has been proven on a lap of the Mugello circuit (Italy), where the longitudinal accelerations are as high as *1 g* and the roll angle exceeds *50°*. The presented virtual rider updates at each instant the control action based on the information of the approaching road section and the current vehicle state. In this manner it mimics the real riders behaviour. Future works will extend the method presented herein to the path and speed following problem.

REFERENCES

[1] V. Cossalter, *Motorcycle Dynamics*, Lulu.com, 2006.

[2] R. S. Sharp, "Stability, control and steering responses of motorcycles", Vehicle Syst. Dyn, **35** (2001) p 291-318.

[3] H. B. Pacejka, *Tyre and Vehicle Dynamics*, Butterworth and Heinemann, Oxford, 2002.

[4] V. Cossalter, M. Da Lio, R. Lot, L. Fabbri, "A general method for the evaluation of vehicle manoeuvrability with special emphasis on motorcycles", *Vehicle Syst. Dyn*. **31** (1999), pp. 113–135.

[5] S. Bobbo, V. Cossalter, M. Massaro, M. Peretto, "Application of the Optimal Maneuver Method for Enhancing Racing Motorcycle Performance", *SAE Int. J. Passeng. Cars – Mech. Syst.* **1** (2009), 1311-1318.

[6] V. Cossalter, R. Lot, "A non linear rider model for motorcycles", *Proc. of the FISITA 2006, World Automotive Congress*, 22-27 October, Yokohama, Japan, 2006.

[7] R. Lot, M. Massaro, R. Sartori, "Advanced motorcycle virtual rider", *Vehicle Syst. Dyn.* **46** (2008), pp. 215-224, DOI:10.1080/00423110801935822.

[8] R. S. Sharp, "Optimal linear time-invariant preview steering control for motorcycles", *Vehicle Syst. Dyn*. **44** (2006), 329 - 340.

[9] R. S. Sharp, "Optimal preview speed-tracking control for motorcycles", *Multibody Syst. Dyn.* **18** (2007), pp. 397–411.

[10] A. Saccon, J. Hauser, A. Beghi, "A Virtual Rider for Motorcycles: An Approach Based on Optimal Control and Maneuver Regulation", *Proc. of the 3rd International Symposium on Communications, Control, and Signal Processing, ISCCSP 2008*, p 243-248, 2008.

[11] S. Rowell, A. A. Popov; J. P. Meijaard, "Application of predictive control strategies to the motorcycle riding task", *Vehicle Syst. Dyn.* **46** (2008), pp. 805–814.

[12] M. Massaro, "A Nonlinear Virtual Rider for Motorcycles", *Vehicle Syst. Dyn.*, (2010) DOI:10.1080/00423114.2010.521843.

[13] V. Cossalter, R. Lot, M. Massaro, "An advanced multibody code for handling and stability analysis of motorcycles", *Meccanica*, (2010), DOI:10.1007/s11012-010-9351-7.

[14] V. Cossalter, A. Doria, R. Lot, M. Massaro, "The effect of rider's passive steering impedance on motorcycle stability: identification and analysis", *Meccanica*, (2010), DOI:10.1007/s11012-010-9304-1.

[15] M. Massaro, R. Sartori, R. Lot, "Numerical Investigation of Engine-to-Slip Dynamics for Motorcycle Traction Control Applications", *Vehicle Syst. Dyn.*, (2010), DOI:10.1080/00423110903530992.

[16] M. Massaro, R. Lot, V. Cossalter, "On Engine-to-Slip Modelling for Motorcycle Traction Control Design", *Journal of Automobile Engineering, part D*, (2010), DOI:10.1243/09544070JAUTO1575.

[17] V. Cossalter, R. Lot, M. Massaro, "The chatter of racing motorcycle", *Vehicle Syst. Dyn*, **46**, (2008), pp. 339-353, DOI:10.1080/00423110701416501.

[18] V. Cossalter, R. Lot, M. Massaro, "The influence of Frame Compliance and Rider Mobility on the Scooter Stability", *Vehicle Syst. Dyn.*, **45** (2007), pp. 315-326, DOI:10.1080/00423110600976100.

[19] J.M. Maciejowski, *Predictive Control: With Constraints*, Prentice-Hall: London, 2002.

[20] V. Cossalter, R. Lot, F. Maggio, "On the Braking Behavior of Motorcycles", *SAE paper 2004-32-0018*, 2004.

[21] F. Biral, R. Lot, "An interpretative model of g-g diagrams of racing motorcycle", *Proc. of the 3rd ICMEM*, October 21−23, 2009, Beijing, P. R. China.

APPENDIX

Table 1. Main vehicle parameters.

whole vehicle mass (vehicle + rider)	*256 kg*
c.g. height (from ground)	*0.640 m*
c.g. longitudinal position (from rear contact point)	*0.710 m*
wheelbase	*1.415 m*
normal trail	*0.091 m*
caster angle	*23.9°*
roll moment of inertia	*18.6 kgm^2*
pitch moment of inertia	*50.5 kgm^2*
yaw moment of inertia	*37.2 kgm^2*
rear wheel mass	*13.0 kg*
rear wheel spin inertia	*0.535 kgm2*
rear tyre radial stiffness	*135 kN/m*
rear tyre lateral stiffness	*120 kN/m*
rear tyre circumferential stiffness	*100 kN/m*
front wheel mass	*11.2 kg*
front wheel spin inertia	*0.456 kgm2*
front tyre radial stiffness	*140 kN/m*
front tyre lateral stiffness	*150 kN/m*
front tyre circumferential stiffness	*100 kN/m*
aerodynamics drag area coefficient (CDA)	*0.5 m2*
height of the aerodynamic centre (from ground)	*0.833 m*
front frame twist stiffness	*45 kNm/rad*
rear suspension stiffness reduced to rear contact point	*21 kN/m*
rear suspension damping reduced (compression)	*928 Ns/m*
rear suspension damping reduced (extension)	*2484 Ns/m*
front suspension stiffness	*18 kN/m*
front suspension damping (compression)	*525 Ns/m*
front suspension damping (extension)	*974 Ns/m*
steering damping coefficient	*5 Nms/rad*

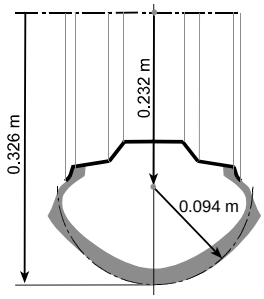

Figure 4. Rear tyre profile (unloaded)**.**

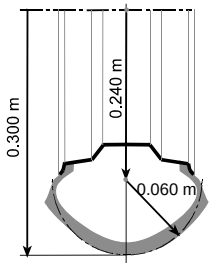

Figure 5. Front tyre profile (unloaded).

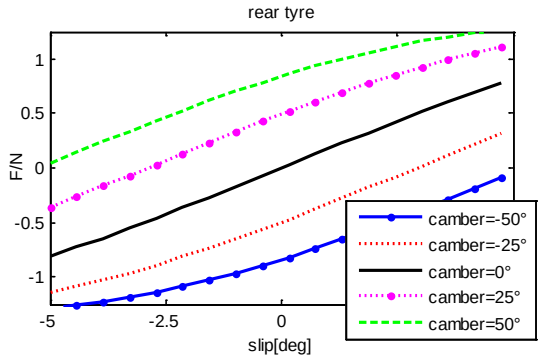

Figure 6. Rear tyre lateral force.

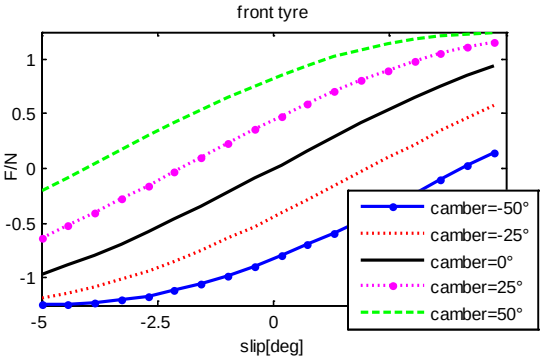

Figure 7. Front tyre lateral force.

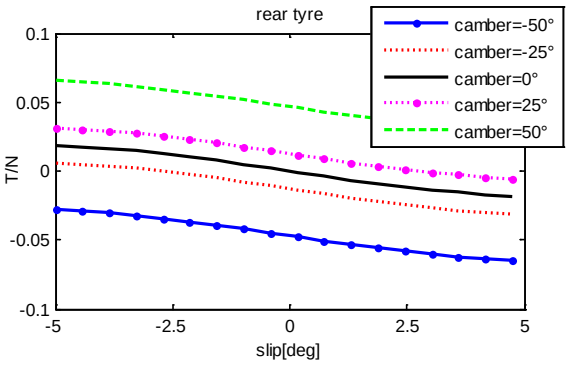

Figure 8. Rear tyre yawing torque.

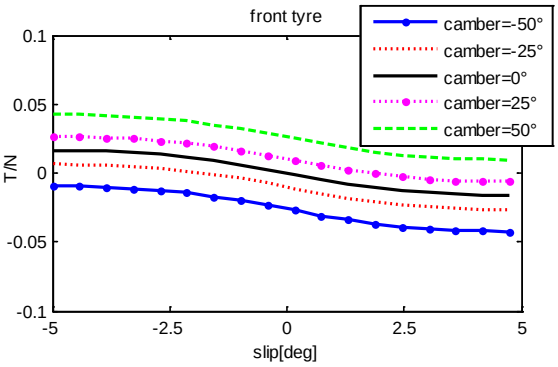

Figure 9. Front tyre yawing torque.

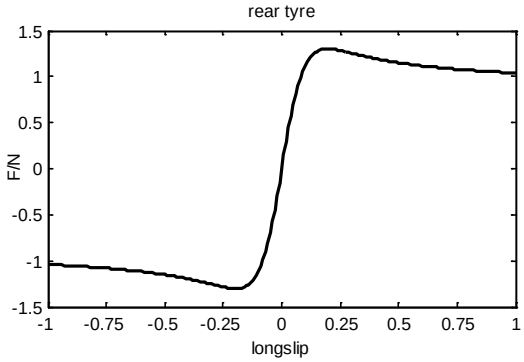

Figure 10. Rear tyre longitudinal force.

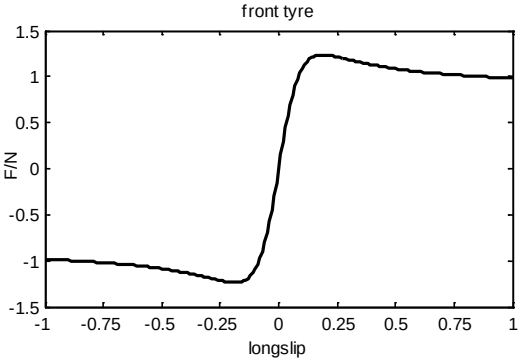

Figure 11. Front tyre longitudinal force.